Commemoration of Zoltan Fried

University of Massachusetts at Lowell

Experimental Gravitation: GPB and other adventures

Rainer Weiss
MIT

October 13, 2004

ELECTRON INTERFERENCE EFFECTS INDUCED BY LASER LIGHT*

John F. Dawson and Zoltan Fried
Lowell Technological Institute, Lowell, Massachusetts
(Received 22 June 1967)

We propose an electron-interference experiment involving laser light. It is estimated (roughly) that presently available (cw) laser sources can yield detectable "fringe" displacement in the electron interference pattern.

The interaction of laser light with free electrons has been the subject of numerous papers.[1,2] All of these involve the effect of the background laser light on Compton scattering. With the exception of the Kapitza-Dirac effect,[1] the deviations from the Klein-Nishina formula due to the presence of the laser light[2] are characterized by the dimensionless parameter ξ. In terms of the fundamental parameters of the problem,

$$\xi = (1/137)\rho\lambda_c^{\,2}\lambda,$$

where ρ is the photon density, λ_c is the electron Compton wavelength, and λ is the wavelength of the laser radiation. Presently available lasers yield small values for the dimensionless parameter ξ ($\sim 10^{-4}$); hence any deviation from the Klein-Nishina formula[2] is difficult to detect. In retrospect, the fact that the change in the phase shift of the electron-photon systems as result of the background light is so small is not really surprising. The change in the Klein-Nishina amplitude[2] as a consequence of the background external field comes about (a) because the incident and final-state electron wave functions contain external-field-dependent phase terms, and (b) because these phases are momentum dependent. This relative phase, which can be detected in a scattering experiment, thus depends on the amount of the momentum transfer. Since in optical experiments with slow electrons the momentum transfer is of the order $\hbar\vec{k}/mc$, the net phase change is small. ($\vec{k}$ is the wave vector of the laser light.)

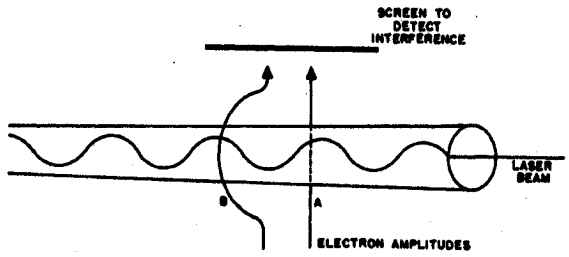

FIG. 1. Schematic for electron-interference experiment.

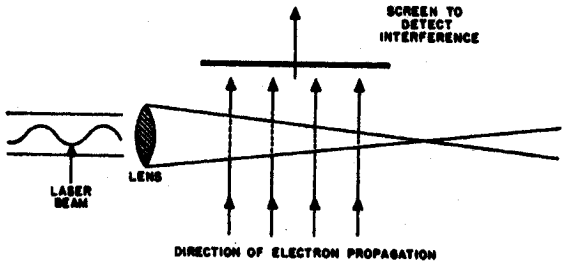

FIG. 2. An alternative way to construct interference.

For a focused (i.e., focused to a diameter of the order of 10^{-4} cm) cw argon laser, this parameter can be as large as unity. All other competing effects, such as Compton scattering (even by induced emission) and harmonic production, are negligible.[7]

Finally, an alternative way to do the experiment (to be sure, there are many more ways) is indicated in Fig. 2. Here the complete electron amplitude propagates through the tapering conical section of the focused laser beam. The interference arises due to the change in the effective "optical" path length of the electron wave function. For a fixed power emanating from the laser, the phase change as a function of the position-dependent diameter is

$$\eta(d) = \frac{e^2}{2mc^2}\frac{\langle A^2\rangle}{\hbar v}\left(\frac{d_0}{d}\right)^2 d, \tag{8}$$

where d_0 is the diameter of the laser beam at the position of the lens.

In summary, we wish to stress that although interference experiments with electrons are harder than scattering experiments (such as Kapitza-Dirac effect), the proposed scheme has the advantage of requiring much smaller intensities.

It is a pleasure to thank Professor Rainer Weiss of MIT for discussions concerning the feasibility of this proposed experiment.

---

*Work supported by U. S. Army Research Office (Durham) and administered by Lowell Technological Institute Research Foundation.

[1]P. L. Kapitza and P. A. M. Dirac, Proc. Cambridge Phil. Soc. 29, 297 (1933).

[2]T. W. B. Kibble, Phys. Rev. 150, 1060 (1966); N. D. Sen Gupta, Phys. Letters 21, 642 (1966); Z. Fried, A. Baker, and D. Korff, Phys. Rev. 151, 1040 (1966); P. Stehle and P. G. De Baryshe, Phys. Rev. 152, 1135 (1966), and numerous references therein.

[3]The difficulty stems from the fact that the exact macroscopic shape of the spatial extent of the laser beam has to be taken into account.

[4]D. M. Volkov, Z. Physik 94, 250 (1936).

[5]The "edge effect," due to the finite spatial extent of the laser beam, may change the value of the phase shift, but not by an order of magnitude.

[6]Admittedly, we are ignoring all fine points here, such as gauge invariance, finite extent of radiation field, etc.

[7]Several authors, notably J. J. Sanderson, Phys. Letters 18, 114 (1965), and T. W. B. Kibble, Phys. Rev. Letters 16, 1054, 1233(E) (1966), have pointed out that drastic "edge effects" take place when a classical electron enters into a region of strong electric field gradient. These considerations do not apply here, however, because the ph

EXPERIMENTAL GRAVITATION

1. *Weak and Strong Principle of Equivalence*

2. *Weak Field Tests of Relativistic Gravitation*

Solar System Measurements – First and Second Order

Binary Pulsar Systems

"Magnetic" Gravitation - Lense/Thirring Effect

3. *Gravitational Wave Astronomy*

Strong Fields

Astrophysics: inventory of the universe

4. *Cosmology*

Large Scale Geometry and Mass distribution

Composition of Mass and Pressure

Primeval Universe: initial conditions and fluctuations

CASE STUDY 1: THE DEFLECTION OF LIGHT

References:

"The Determination of Einstein's Light-Deflection in the Gravitational Field of the Sun" H. von Klüber in *VISTAS IN ASTRONOMY* V3, 47 (1960)

"A Confirmation of Einstein's General Theory of Relativity by Measuring the Bending of Microwave Radiation in the Gravitational Field of the Sun" E.B. Fomalont and R.A. Sramek , *Astrophysical Journal* V199,749 (1975)

"Further Experimental Tests of Relativistic Gravity Using the Binary Pulsar PSR 1913 + 16" J.H. Taylor and J. M. Weisberg, *Astrophysical Journal* V345, 434 (1989)

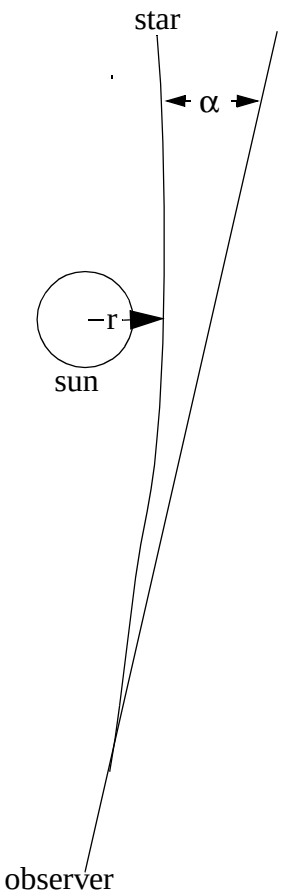

$$\alpha = \frac{4GM}{rc^2}$$

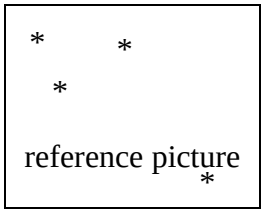

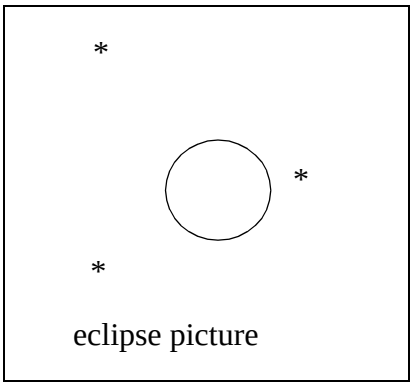

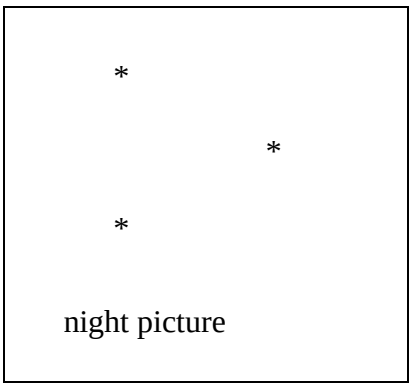

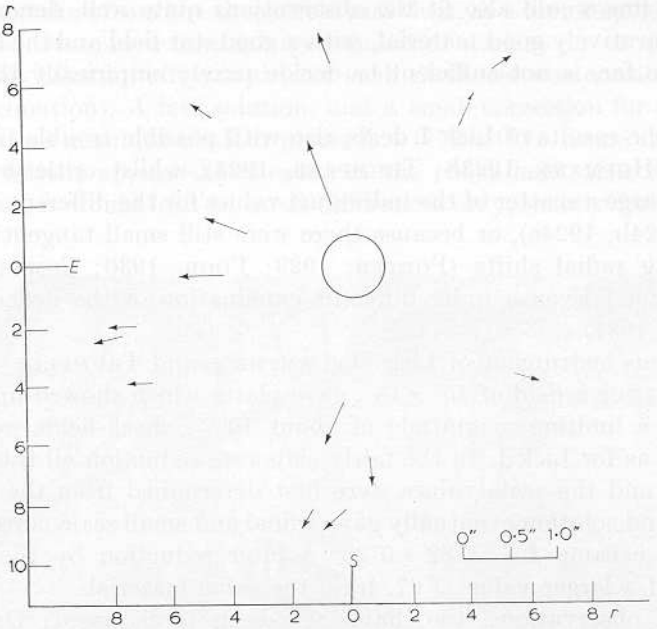

FIG. 9. Vector diagram of the radial shifts, derived from means of the 15 best stars by the Lick I and Lick II observations in 1922. It presents a very good indication of the existence of the light-deflection (CAMPBELL and TRUMPLER, 1928)

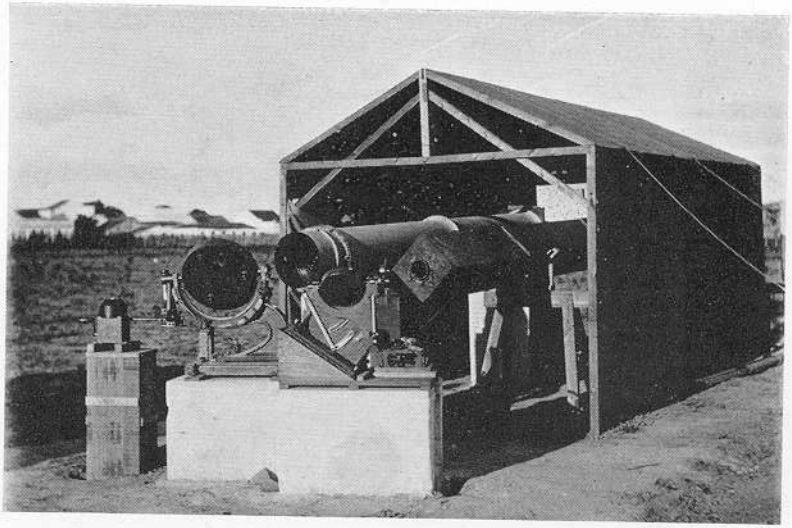

FIG. 7. The instrument used by the Greenwich expedition in 1919 at Sobral (Brazil). The two coelostats are feeding two horizontal telescopes: $f = 343$ cm and aperture 20 cm, on the left; $f = 570$ cm and 10 cm aperture, on the right; DYSON, EDDINGTON and DAVIDSON, 1920. (Photo. C. R. DAVIDSON.)

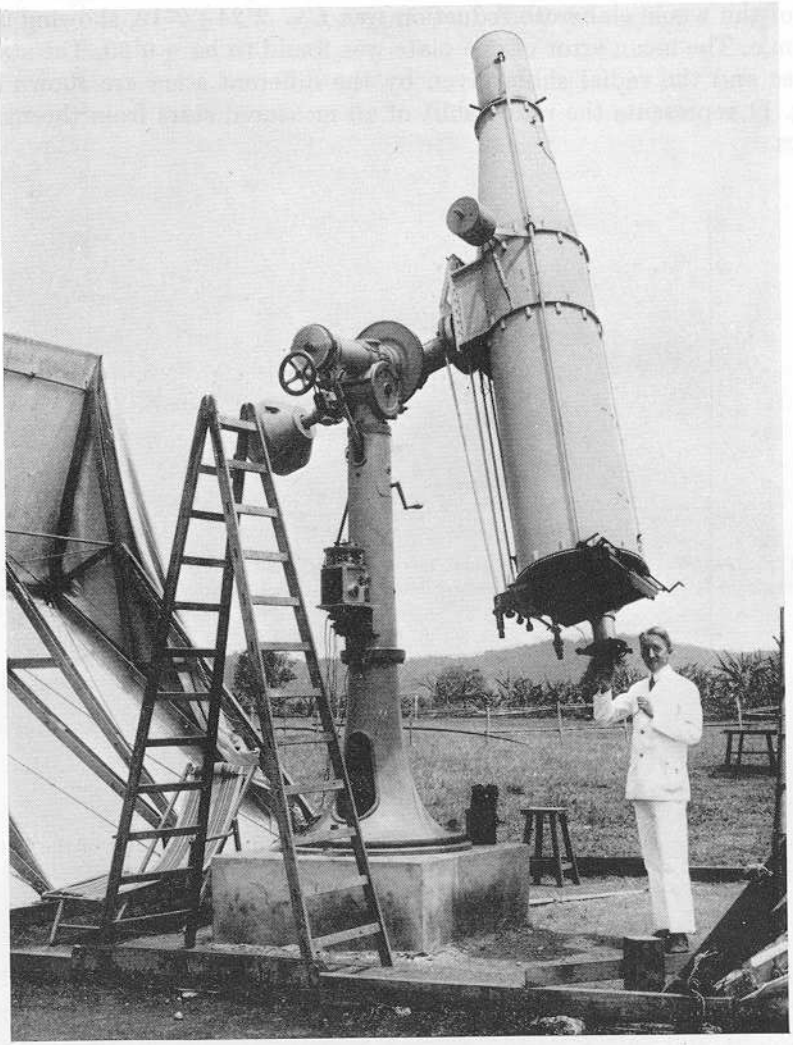

FIG. 12. Large parallactically mounted Zeiss astrograph ($f = 343$ cm, 20 cm aperture) with electrically controlled automatic drive, covering the large field of $7^{\circ}5 \times 7^{\circ}5$, as used in 1929 by the Potsdam observers (Potsdam II). During the eclipse itself a check star-field was photographed on each of the three plates taken of the Sun's surrounding, by pointing the astrograph alternately at a star-field distant from the Sun (FREUNDLICH, v. KLÜBER, v. BRUNN, 1933). (Photo: v. KLÜBER.)

Table 1

1	2	3	4	5	6	7	8	9	10	11	12	13	14	15	16	17	18
	Observatory (site)	Eclipse	Focal length f (cm)	Aperture ϕ (cm)	ϕ/f	Instrument (lens)	Field of plate	Number of plates	Exposure (sec)	Limiting stellar magnitude	Number of stars	r_{min} (solar radii from centre)	r_{max} (solar radii from centre)	Check-field	L	m.s.e.	Reference
1	Greenwich (Brazil)	1919 May 29	570	10	1:57	Coelostat (Double)	2°4x2°0	7	28	6(ph)	7	2	6	no	1″.98	0″.16	DYSON-EDDINGTON-DAVIDSON, 1920
			343	20	1:17	Coelostat (Double)	2·7×2·7	16	5–10	6(ph)	11	2	6	no	0·93	—	
2	Greenwich (Principe)	1919 May 29	343	20	1:17	Coelostat (Double)	2·7×2·7	2	2–20	6(ph)	5	2	6	no	1·61	0·40	
3	Adelaide-Greenwich (Australia)	1922 Sept. 21	160	7·5	1:21	Astrograph (Quadruple)	7×8	2	20–30	8·3	11–14	2	10	yes	1·77	0·40	DODWELL-DAVIDSON, 1924
4	Victoria (Australia)	1922 Sept. 21	330	15	1:22	Astrograph (Quadruple)	—	2	45	9·0	18	2	10	not used	1·75 1·42 2·16	—	CHANT-YOUNG, 1924.
5	Lick I (Australia)	1922 Sept. 21	450	12	1:37	Doubl. Astrograph (Double)	5×5	4	120–125	10·5(ph)	62–85	2·1	14·5	yes	1·72	0·15	CAMPBELL-TRUMPLER, 1923a.
6	Lick II (Australia)	1922 Sept. 21	150	10	1:15	Astrograph (Quadruple)	15×15	6	60–102	10·4(ph)	145	2·1	42	yes	1·82	0·20	CAMPBELL-TRUMPLER, 1928
7	Potsdam I (Sumatra)	1929 May 9	850	20	1:42	Coelostat (Double)	3×3	4	40–90	8·9	17–18	1·5	7·5	yes	2·24	0·10	FREUNDLICH-v. KLÜBER-v. BRUNN, 1931a.
8	Potsdam II (Sumatra)	1929 May 9	343	20	1:17	Astrograph (Triplet)	7·5×7·5	3	14–56	9·5	84–135	4	15	yes	—	—	FREUNDLICH-v. KLÜBER-v. BRUNN, 1933.
9	Sternberg (U.S.S.R.)	1936 June 19	600	15	1:40	Astrograph (Double)	3·5×3·5	2	25–35	9·6	16–29	2	7·2	not used	2·73	0·31	MIKHAILOV, 1949.
10	Sendai (Japan)	1936 June 19	500	20	1:25	Coelostat (Double)	2·9×2·9	2	80	8·6 (vis.)	8	4	7	no	2·13 1·28	1·15 2·67	MATUKUMA, 1940a.
11	Yerkes I (Brazil)	1947 May 20	609	15	1:40	Astrograph (Triplet)	4×4	1	185	10·2	51	3·3	10·2	not used	2·01	0·27	VAN BIESBROECK, 1949.
12	Yerkes II (Sudan)	1952 Feb. 25	609	15	1:40	Astrograph (Triplet)	4×4	2	60–90	8·6	9–11	2·1	8·6	yes	1·70	0·10	VAN BIESBROECK, 1953

FIG. 6. These 9 combined diagrams show the actually measured light-deflections for each star, as far as available, using only the data given by the authors themselves, without having regard to individual weights or group-means. Some small amendments, mainly due to scale correction, may have to be applied to the one or the other of these observational sets. The broken hyperbola represents the Einstein Effect as it should be expected from theory.

Abscissae: distances from the centre of the Sun in solar radii.

Ordinates: measured light-deflections in seconds of arc.

Inserted into the top right corners are the corresponding star fields, to a distance of about 8 solar radii from the Sun's centre. Only actually measured stars are plotted, without regard to the weight given by the observers. Co-ordinates are indicated, giving the positions of the Sun's centre for 1855·0 (B.D.-charts).

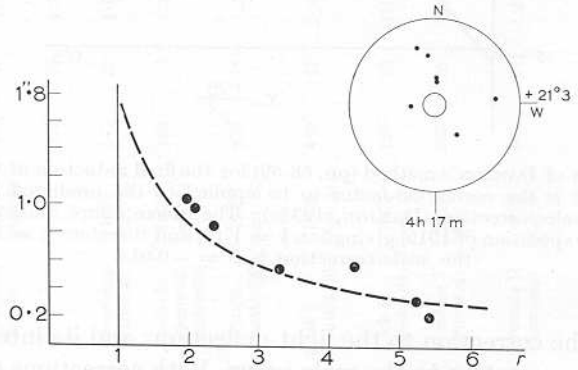

1919 Greenwich, (see Table 1, Nos. 1 and 2)

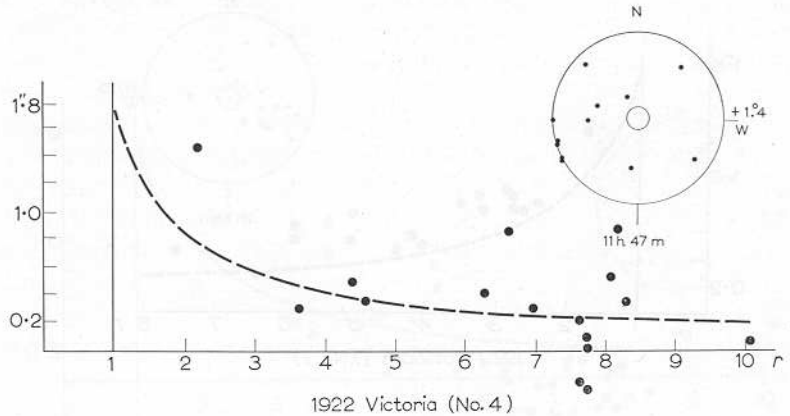

1922 Victoria (No. 4)

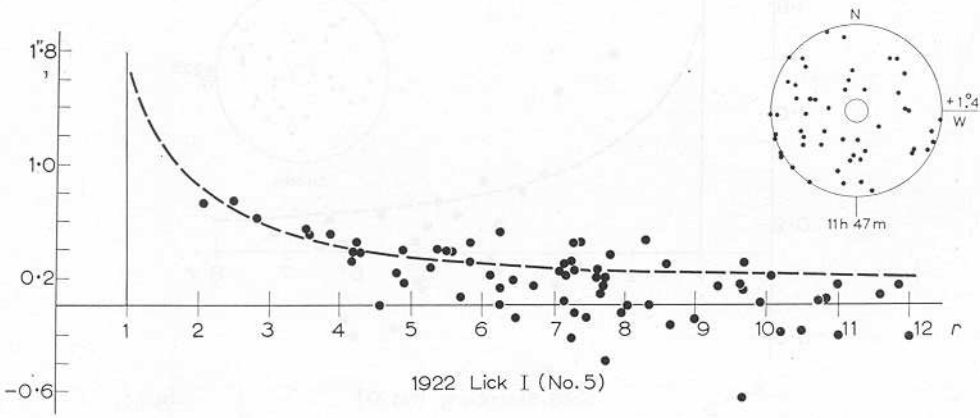

1922 Lick I (No. 5)

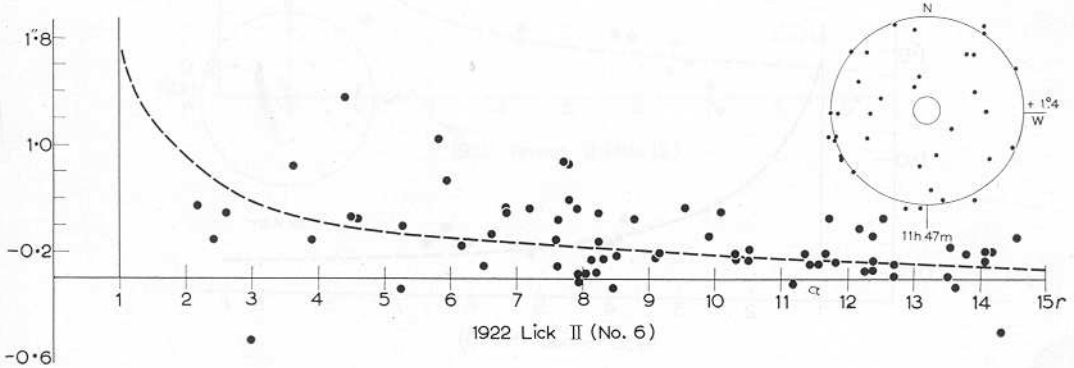

1922 Lick II (No. 6)

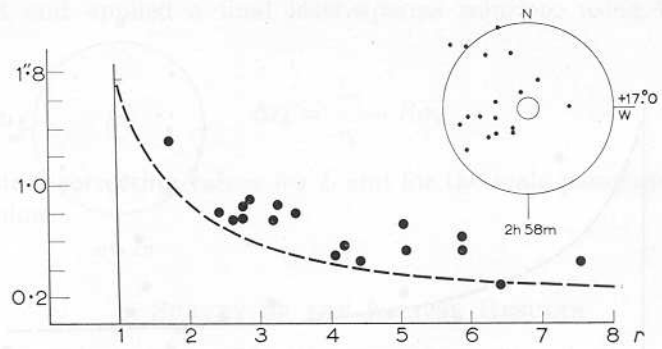

1929 Potsdam I.(No 7)

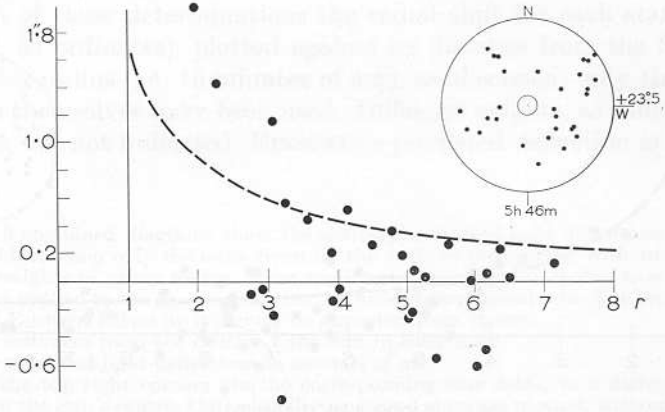

1936 Sternberg (No 9)

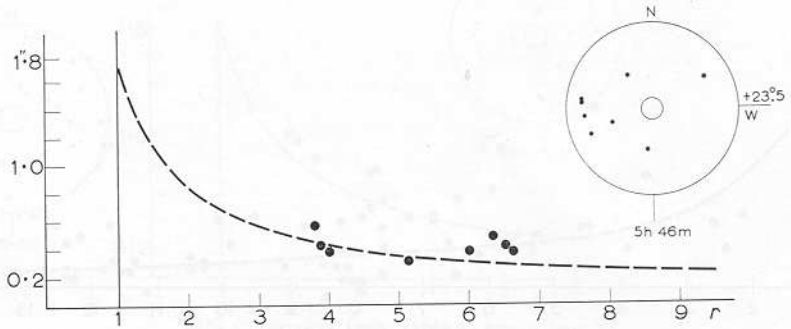

1936 Sendai (No 10)

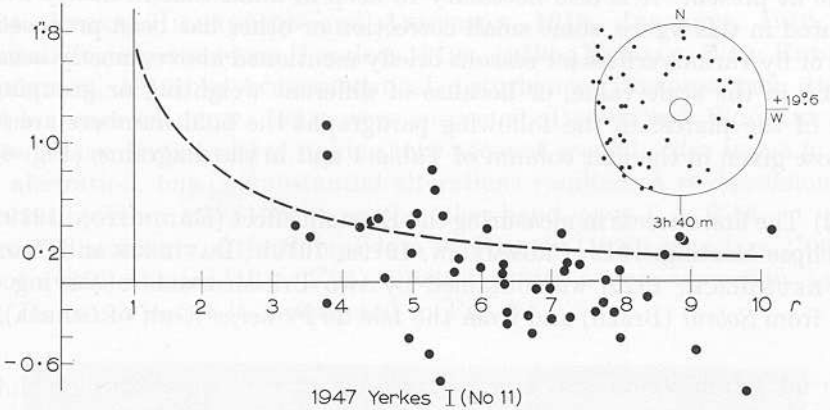

1947 Yerkes I (No 11)

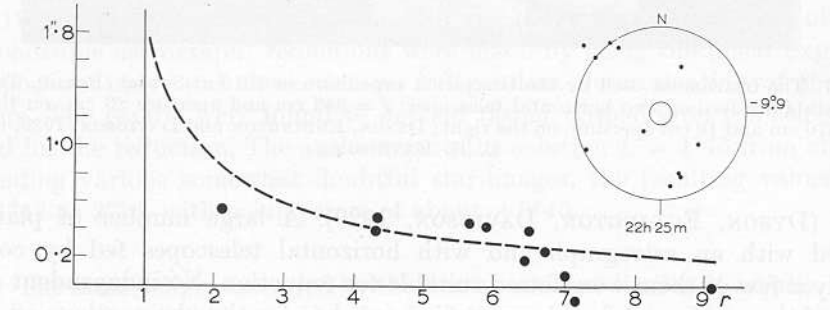

1952 Yerkes II (No. 12)

Fitting procedure for difference between stellar positions in the plates

relative translation
relative rotation
inclination of each plate relative to the telescope optic axis
scale value (magnification)
light deflection

Most significant difficulty - maintaining the scale

30% measurement @ r = 5 $\longrightarrow$ $\Delta\alpha = 0.1\text{sec}$

$$\frac{\Delta f}{f} = \frac{\Delta L}{L} \leq 4\times10^{-6}$$

Inevitable thermal instabilities during the eclipse

Other difficulties

Not enough bright stars within the significant fitting region to separate scale from deflection.
Not enough observing time: 90 minutes total 1919 - 1960

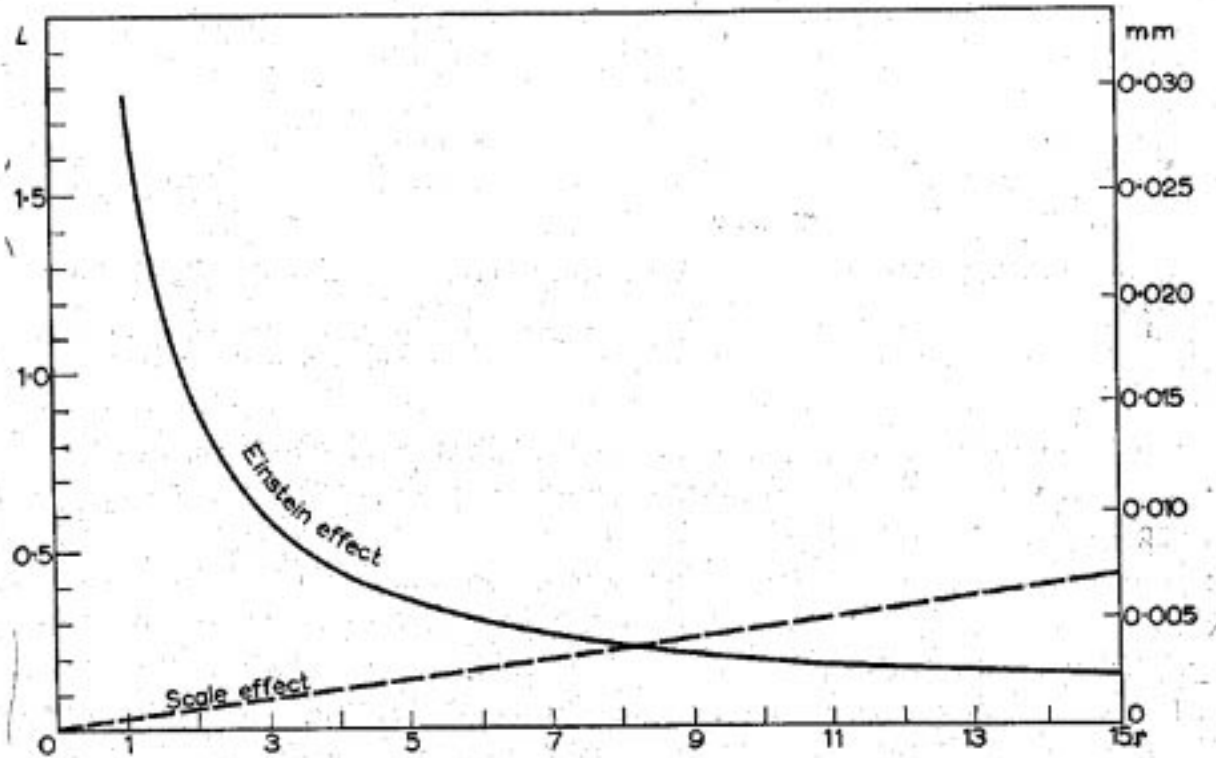

FIG. 2. This graph, a hyperbola, shows the behaviour of the predicted light-deflection, plotted as a function of the distance r from the centre of the Sun. The broken straight line indicates the "Scale Effect" (see p. 53), produced by an alteration of 0·1 mm in the focal setting of a "Normal Astrograph" ($f = 343$ cm).

Abscissae: distances from the centre of the Sun, expressed in units of the solar radius.
Left-hand ordinate: light-deflections in seconds of arc, as predicted by EINSTEIN (1916). See eq. (2).
Right-hand ordinate: the same, but expressed in millimetres on the photophraphic plate, assuming the focal length of the telescope to be 343 cm.

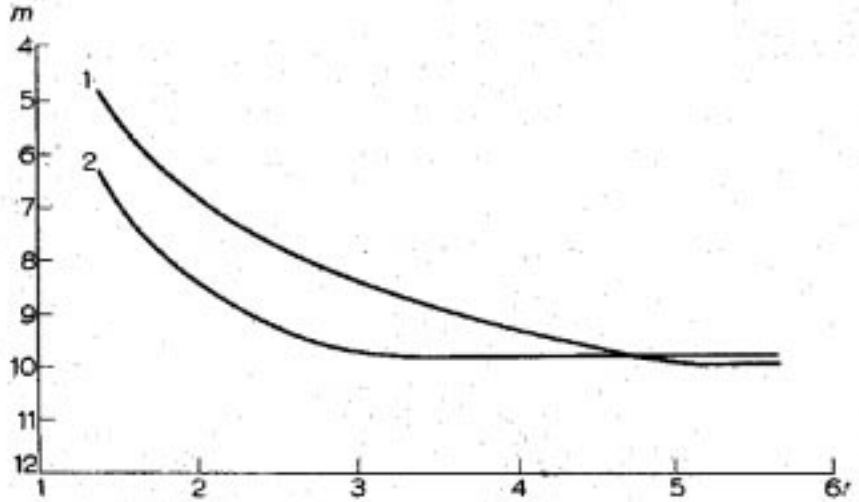

FIG. 3. This diagram indicates in a general manner the faintest stellar magnitude m which may on the average, be recorded on an eclipse photograph, taken with 60 seconds exposure time under favourable conditions, plotted as a function of the distance r of the star from the Sun's centre. (1) Telescope of 20 cm aperture and focal length $f = 343$ cm; (2) telescope of 20 cm aperture and $= 850$ cm. *Abscissae*: distances from the centre of the Sun in solar radaii. *Ordinates*: faintest stellar magnitude to be expected. (v. KLÜBER, 1932b).

BENDING BY MICROWAVE INTERFEROMETRY

λ = 3.7, 11.1 cm

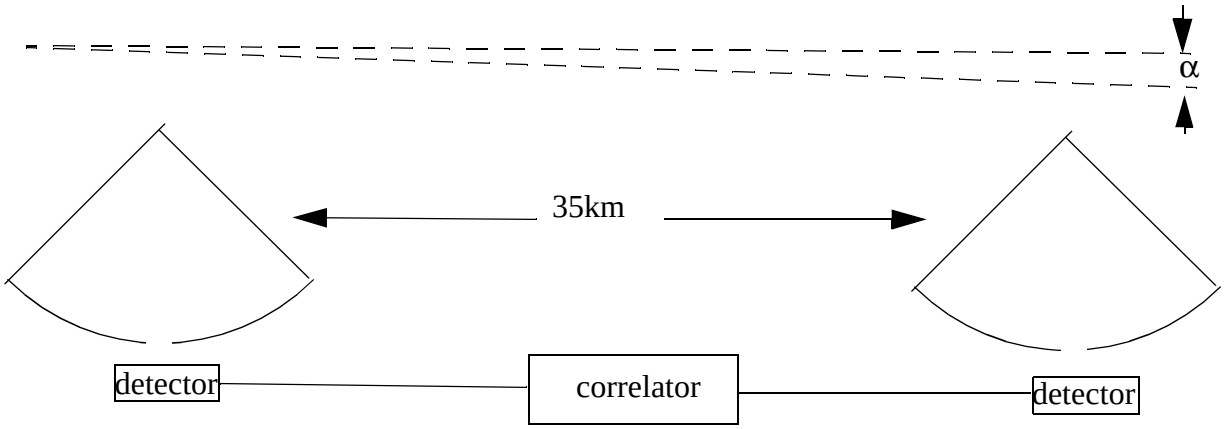

Sensitivity:

$$\Delta\alpha \approx \frac{\lambda}{L} = 1\times10^{-5} = 2 \text{seconds of arc}$$

Split fringe to 0.004 arc seconds in 8 hours of observation

Perturbations

Solar plasma: refraction varies as $\frac{1}{\omega^2}$. Separate by using two different wavelengths

Atmospheric propagation

Control

Measure relative motion of 0116+08, 0119+11 and 0111+02

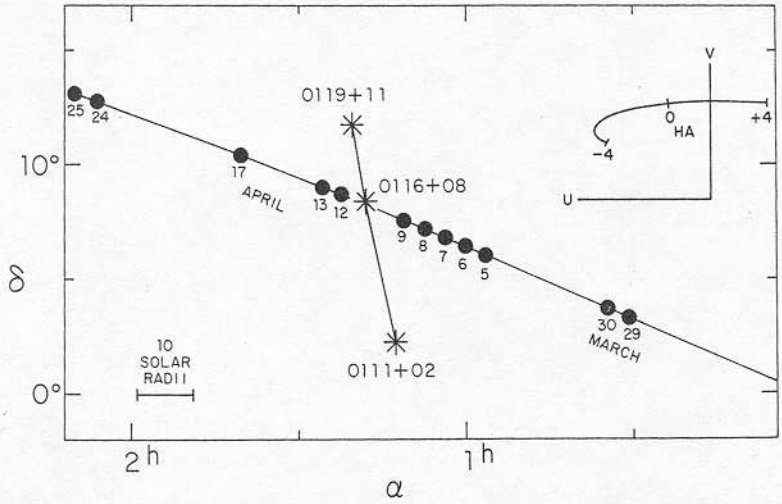

FIG. 1.—The 1974 experiment. The position of the three radio sources and the position of the Sun at noon on each observing day are shown. The coordinates refer to the epoch of date. The projected resolution of the interferometer with hour angle (HA) is given by the (u-v) plot in the upper right.

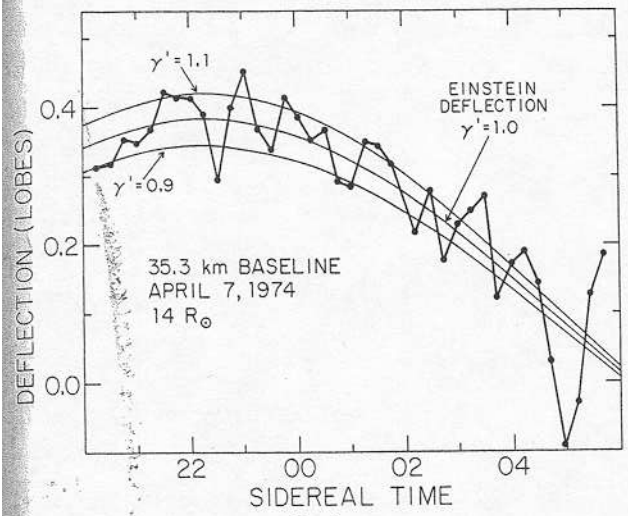

FIG. 3a

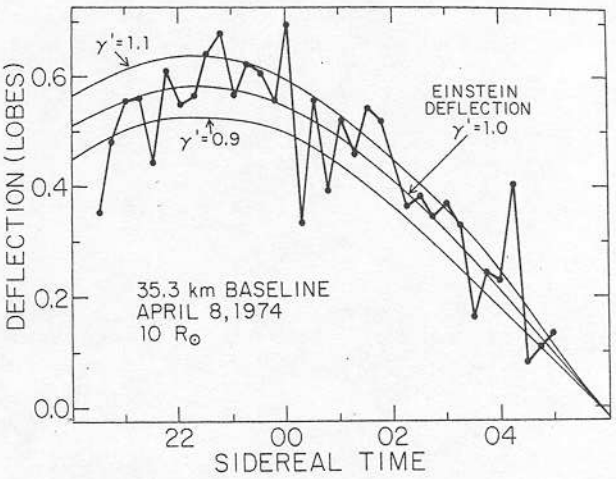

FIG. 3b

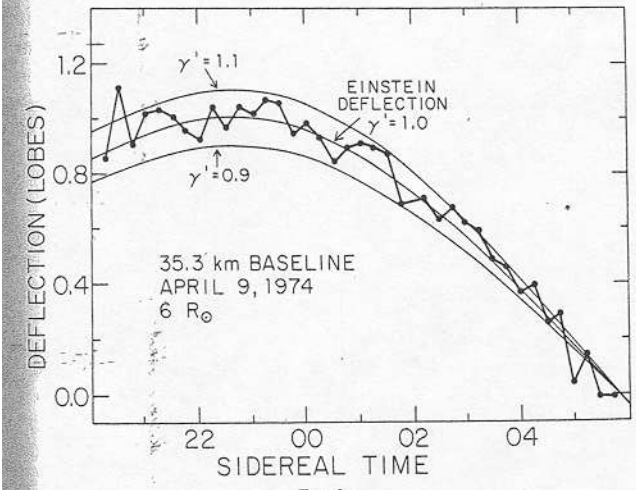

FIG. 3c

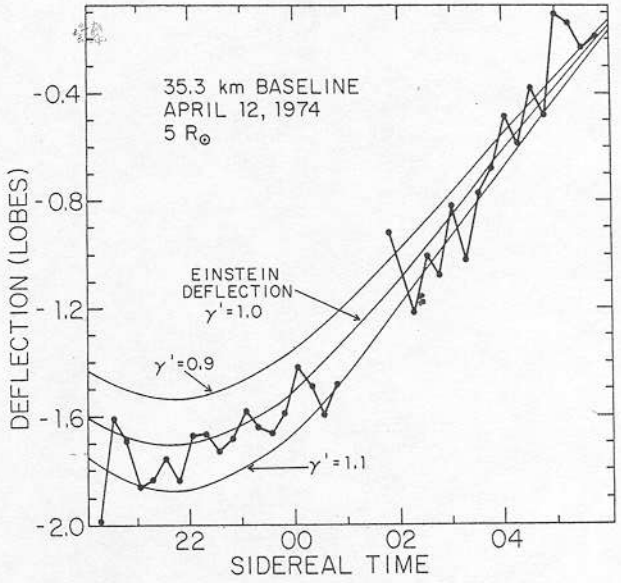

FIG. 3d

FIG. 3.—The measured corrected phase compared with the phase expected for various deflections for (*a*) April 7, (*b*) April 8, (*c*) April 9, and (*d*) April 12. All plots are for the 35.3 km baseline, left-hand polarization. The approximate distance of 0116+08 from the Sun is also given. The average phase for each determination every 15 minutes is shown by the dots.

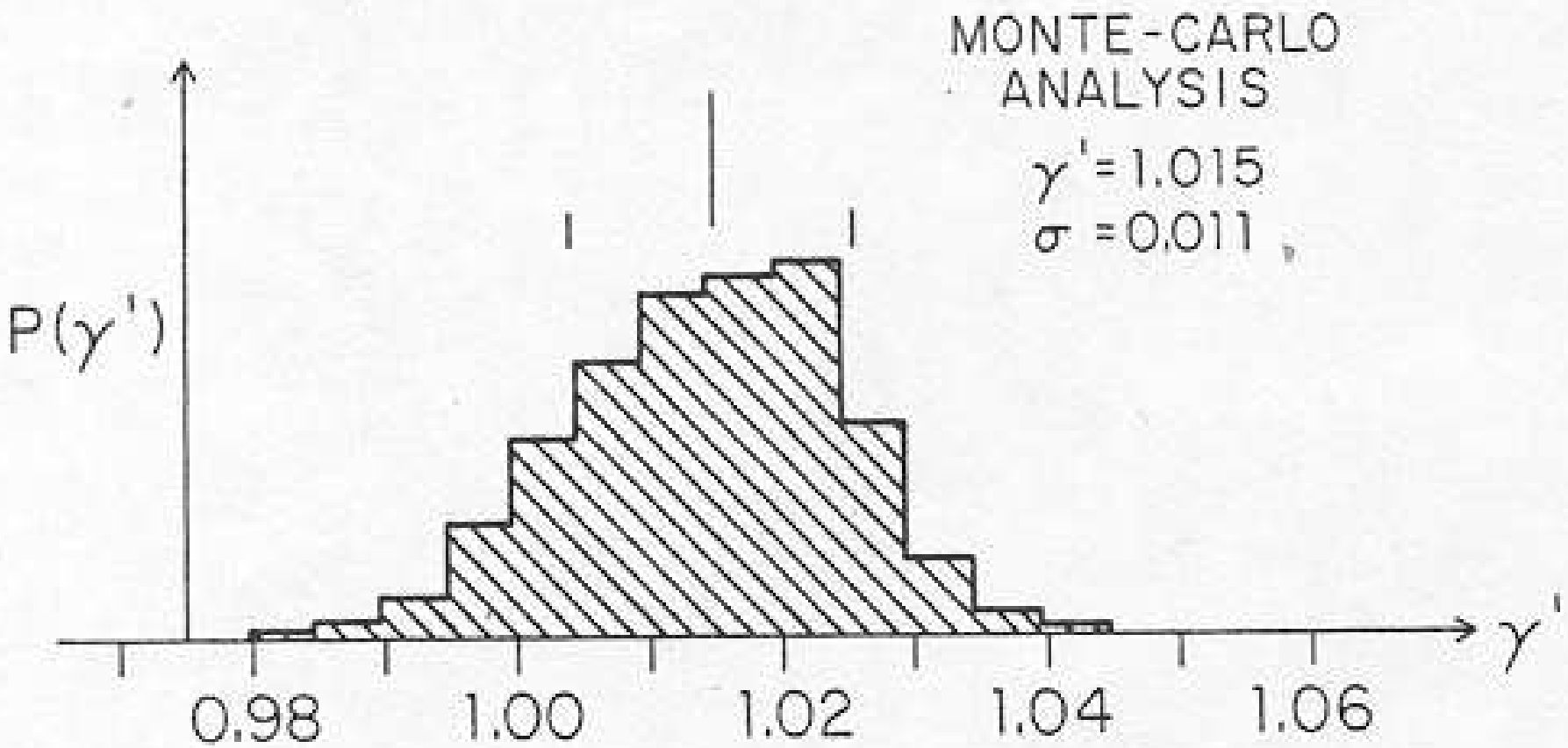

FIG. 4.—The distribution of γ', the coefficient of bending, based on a Monte Carlo analysis of the residual data. The skewness in the distribution is real and reflects the skewness of the distribution of γ' in Table 2. Only the range, not the value, of γ' was determined by this analysis.

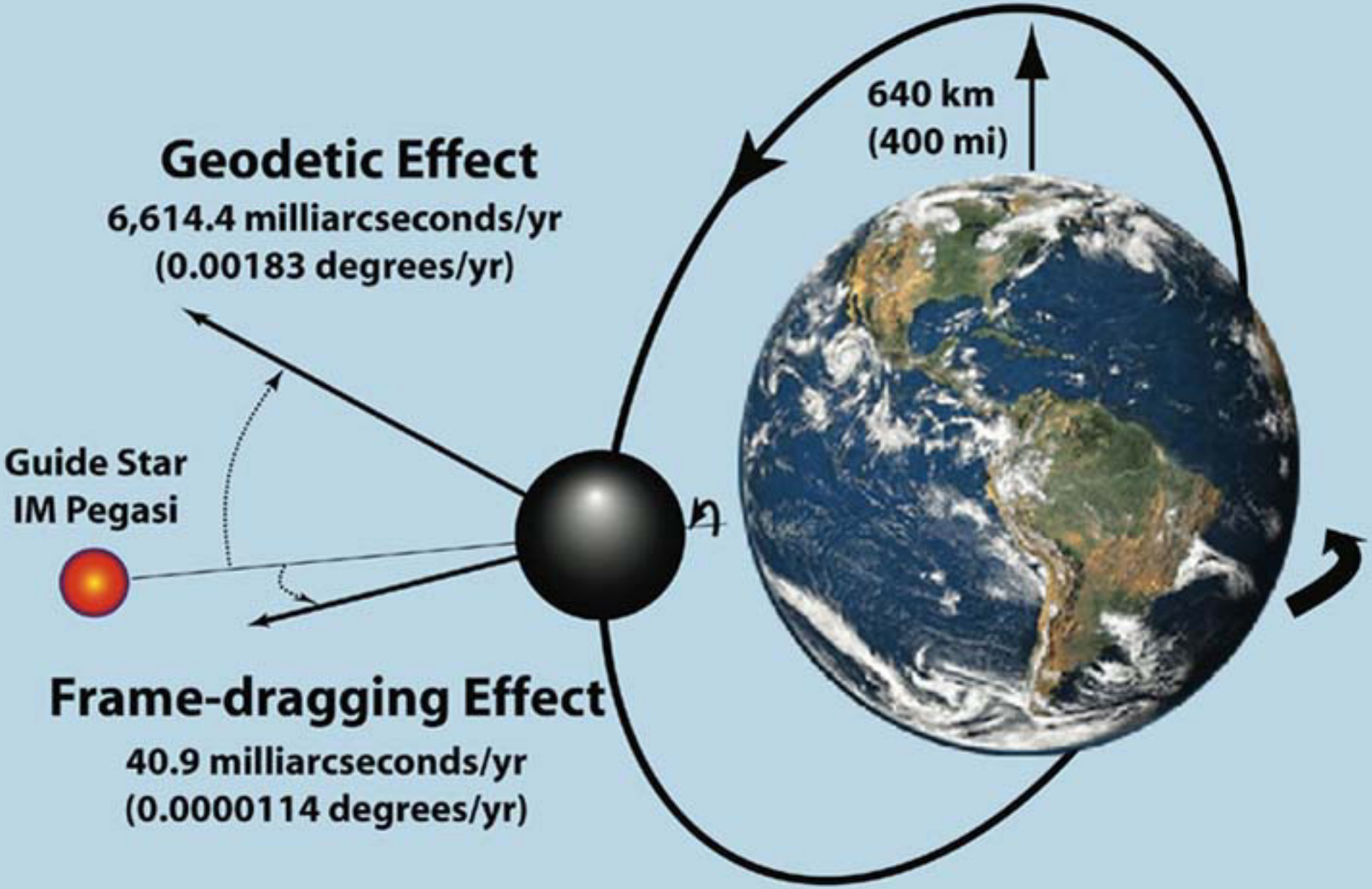
640 km
(400 mi)
Geodetic Effect
6,614.4 milliarcseconds/yr
(0.00183 degrees/yr)
Guide Star
IM Pegasi
Frame-dragging Effect
40.9 milliarcseconds/yr
(0.0000114 degrees/yr)

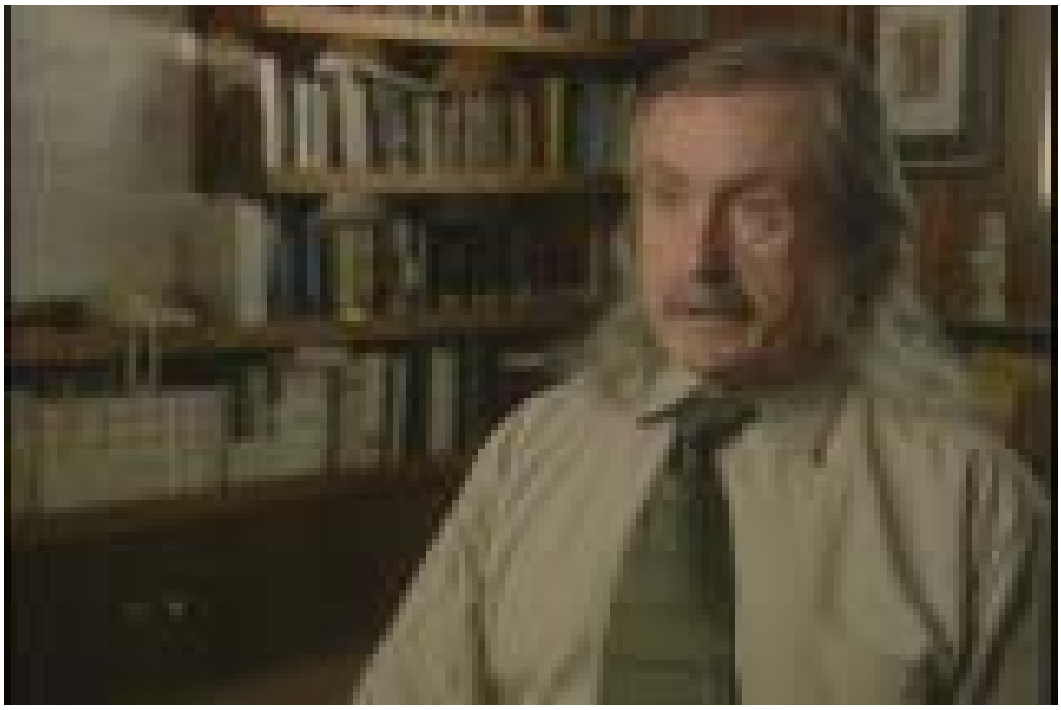

Francis Everitt

Brad Parkinson

GP-B PRIMARY EXPERIMENTS

- **FRAME-DRAGGING Ω_F**

$$\Omega_F = \frac{G\,I}{c^2\,R^3}\left[\frac{3\,\vec{R}}{R^2}\left(\vec{\omega}\cdot\vec{R}\right) - \vec{\omega}\right]$$

MEASURED TO 0.3%

- **GEODETIC EFFECT Ω_G**

$$\Omega_G = \frac{1}{2}\left(1+2\gamma\right)\frac{G\,M}{c^2\,R^3}\left[\vec{R}\times\vec{v}\right]$$

γ – PPN SPACE CURVATURE COEFFICIENT

GEODETIC MEASUREMENT MORE PRECISE BY FACTOR OF 100 THAN ANY PREVIOUS TEST OF GENERAL RELATIVITY

WITHIN PPN FRAMEWORK FIXES $\gamma \sim 2$ PARTS IN 10^5 COMBINED WITH IMPROVED LUNAR RANGING DATA (IF AVAILABLE) FIXES β TO 5 PARTS IN 10^6

GP-B Measurement Concept

ΔGyro Pointing =
ΔTelescope Pointing- ΔStar
(2 axes resolved by roll telescopes)

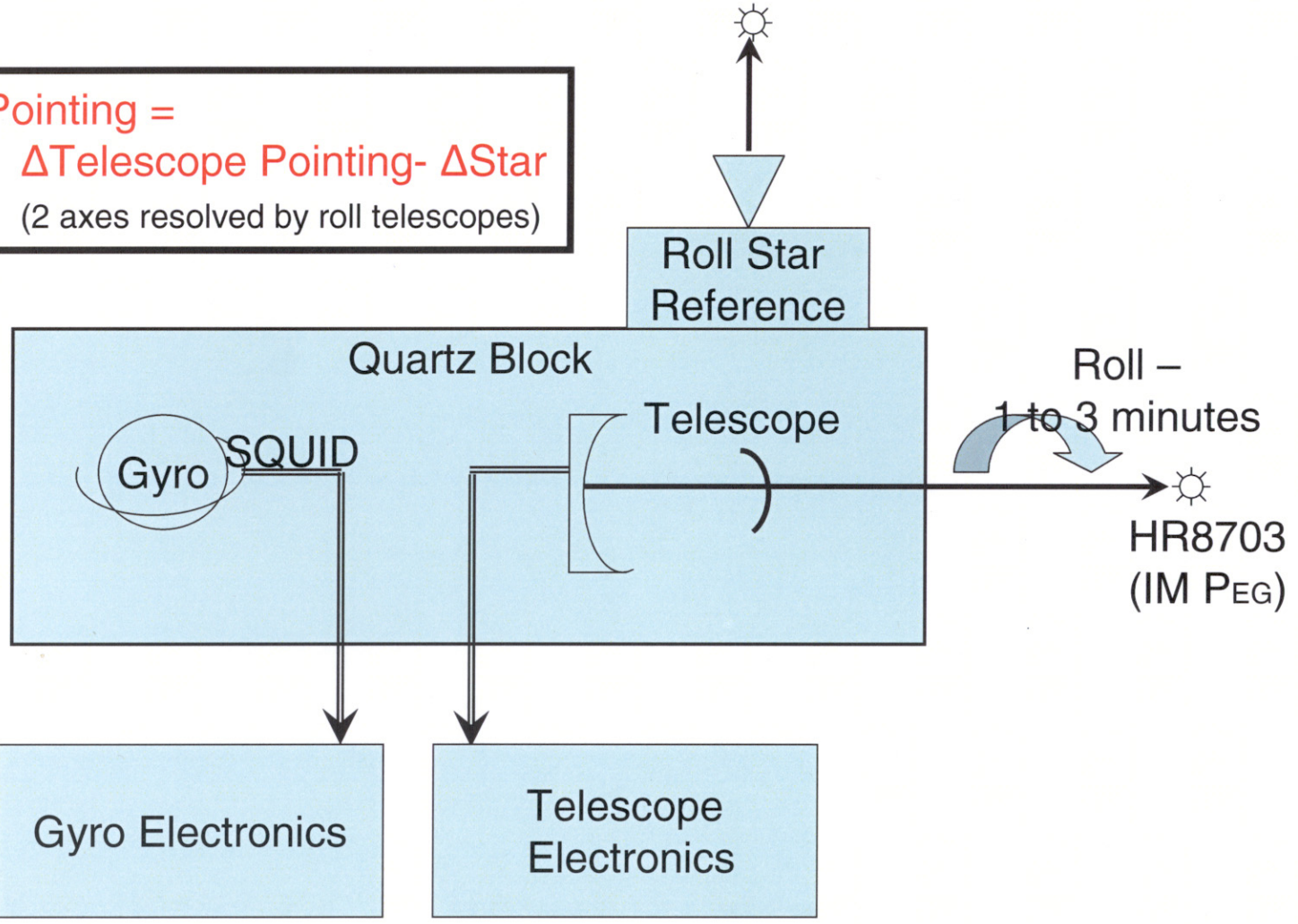

National Aeronautics and
Space Administration

The World's Roundest Gyroscopes

Gravity ProBe

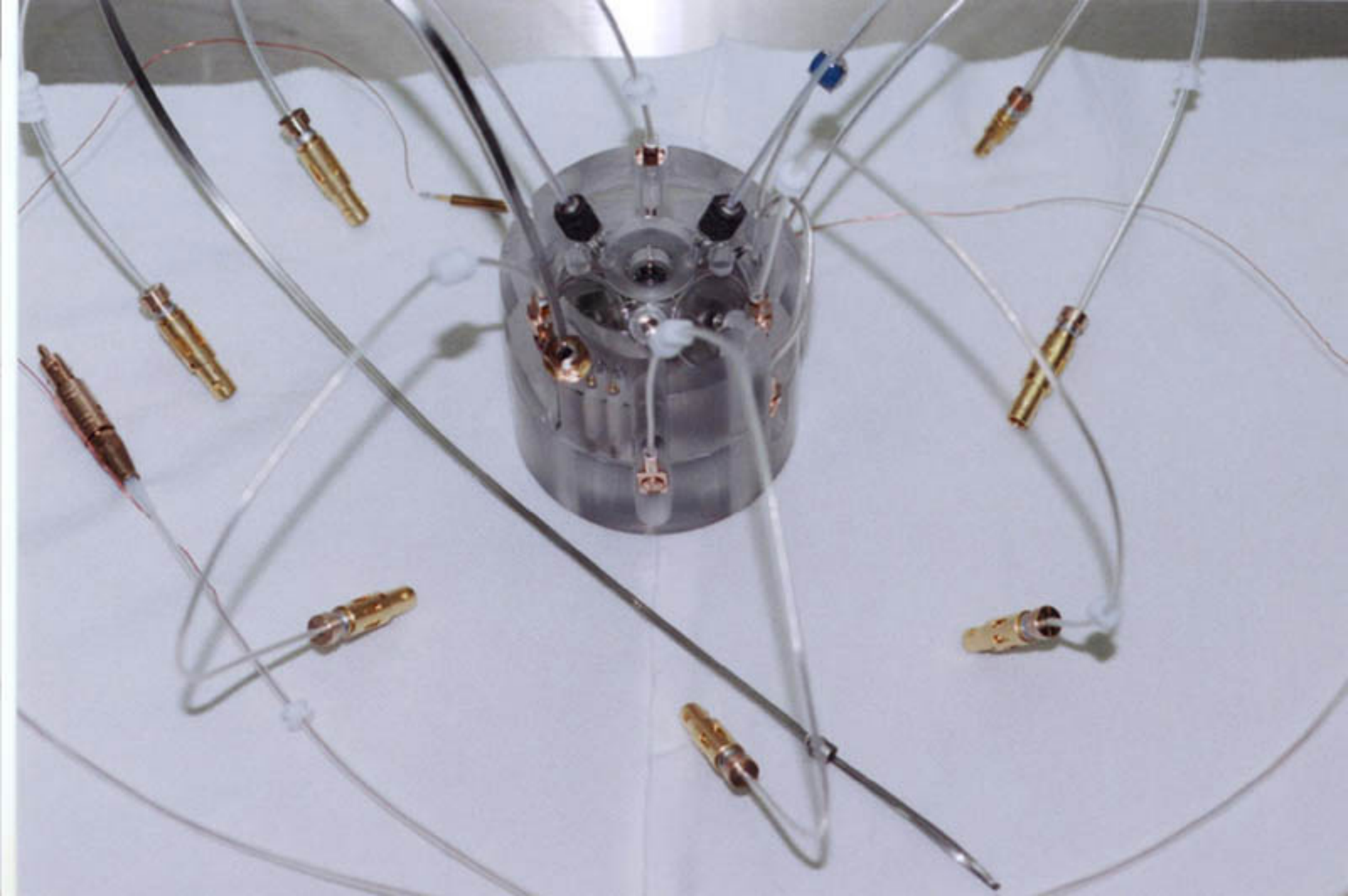

National Aeronautics and Space Administration

Using Superconductivity to "See" A Spin Axis

Gravity ProBe

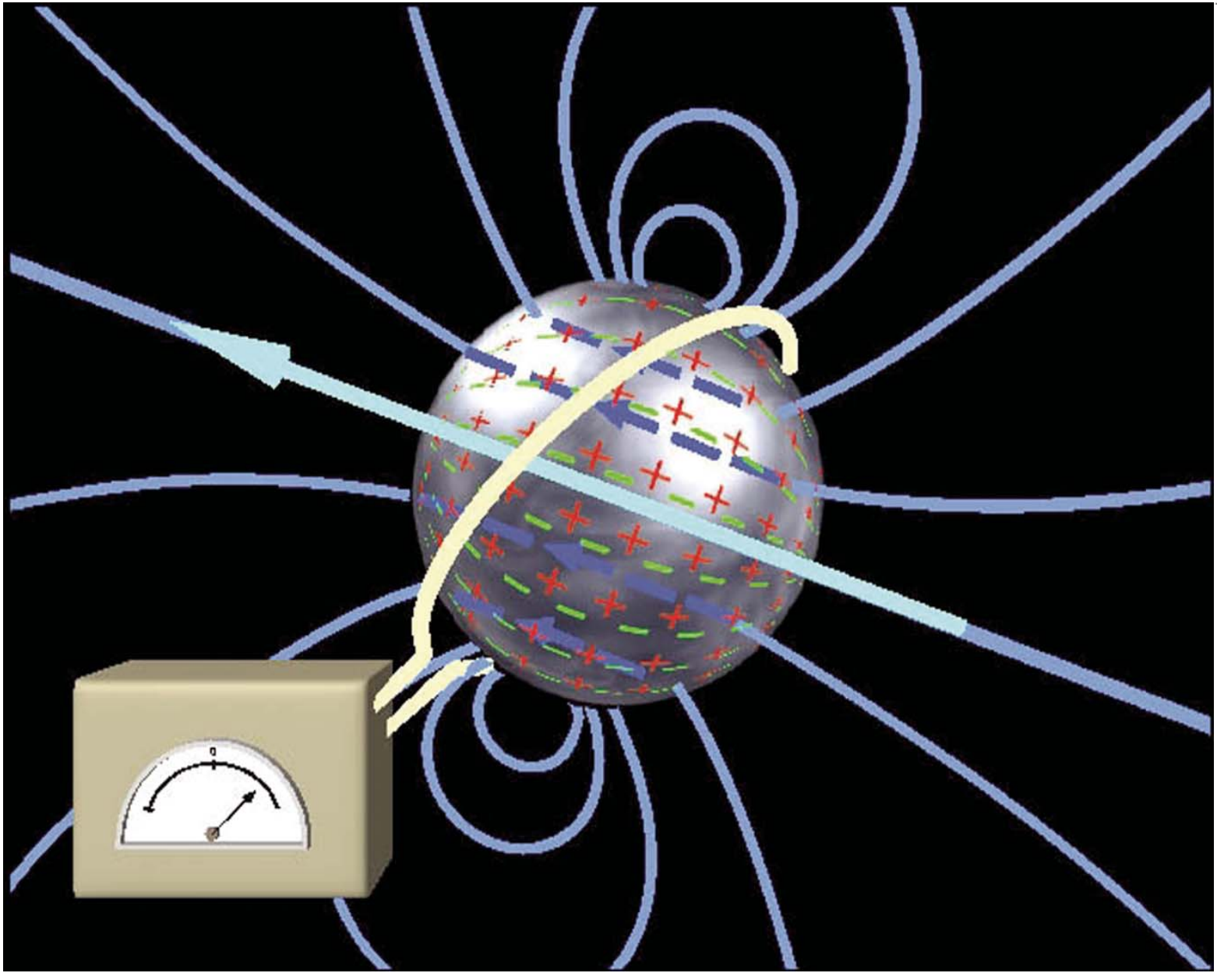

National Aeronautics and
Space Administration

Focusing On the Guide Star

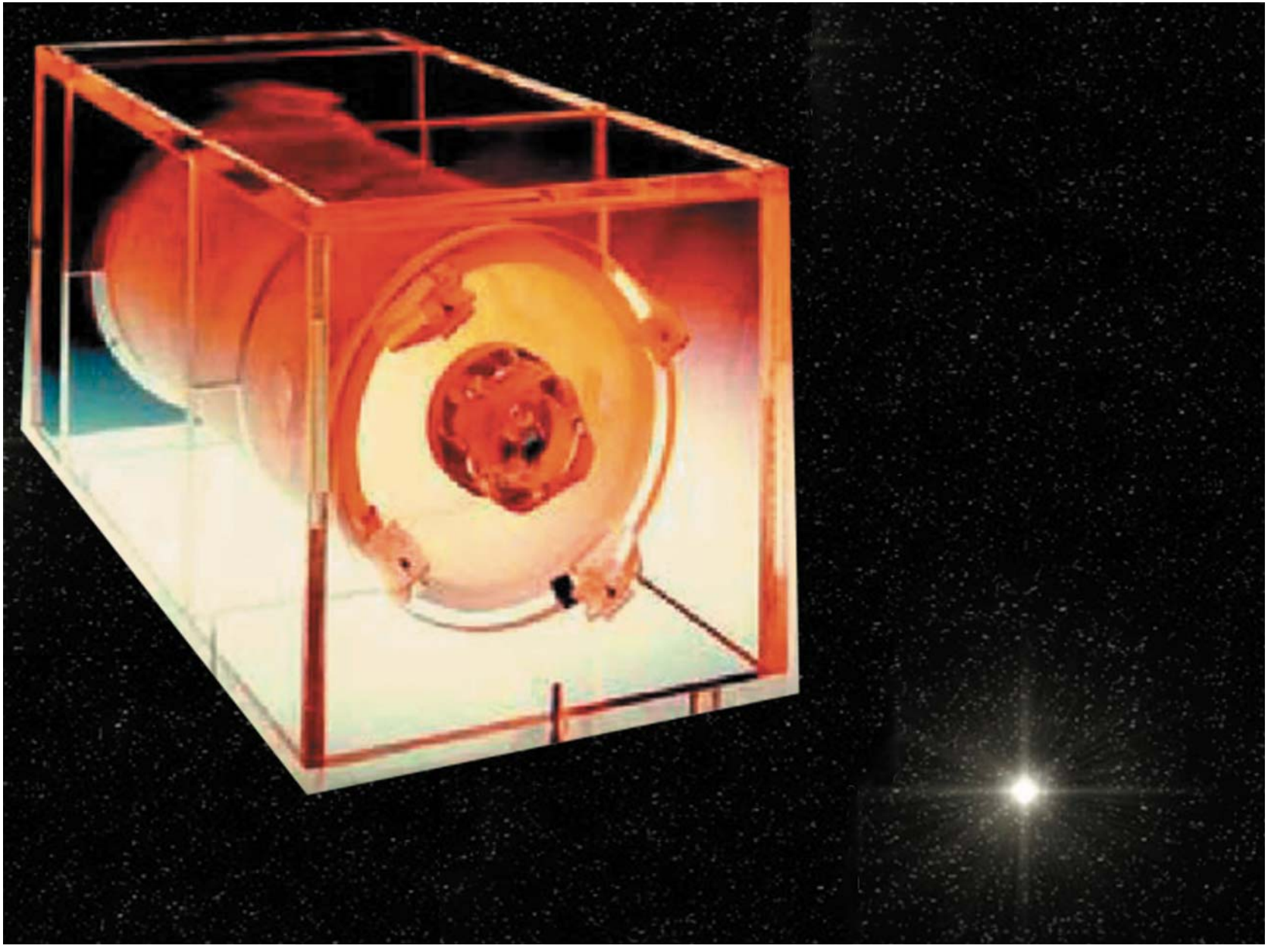

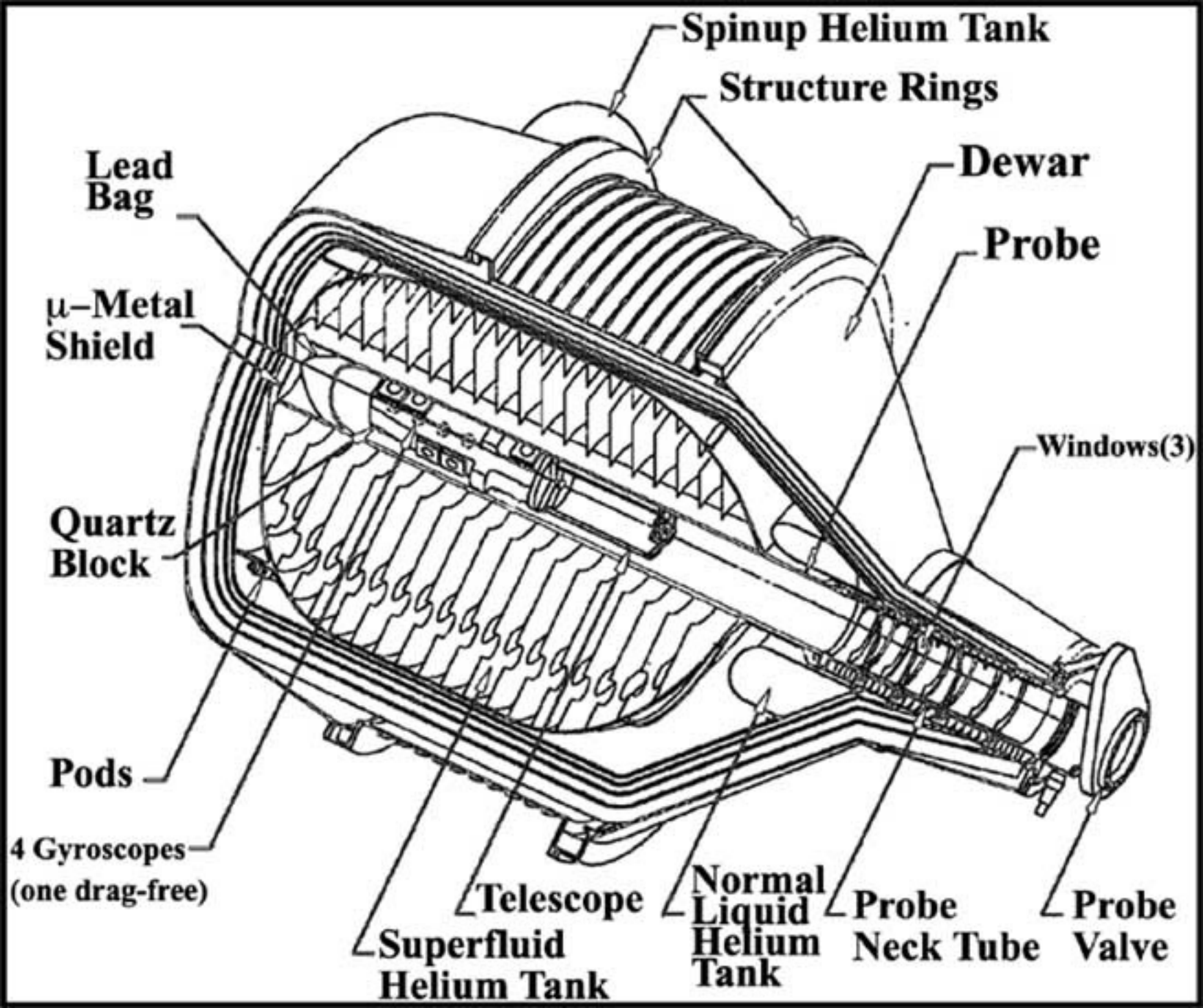
Spinup Helium Tank
Structure Rings
Lead Bag
Dewar
Probe
μ–Metal Shield
Windows(3)
Quartz Block
Pods
4 Gyroscopes (one drag-free)
Telescope
Normal Liquid Helium Tank
Probe Neck Tube
Probe Valve
Superfluid Helium Tank

Frame-dragging: Top Eight Classical Gyro Disturbance Terms *(ALL TERMS > 0.001 MILLIARC-SEC/YEAR)*

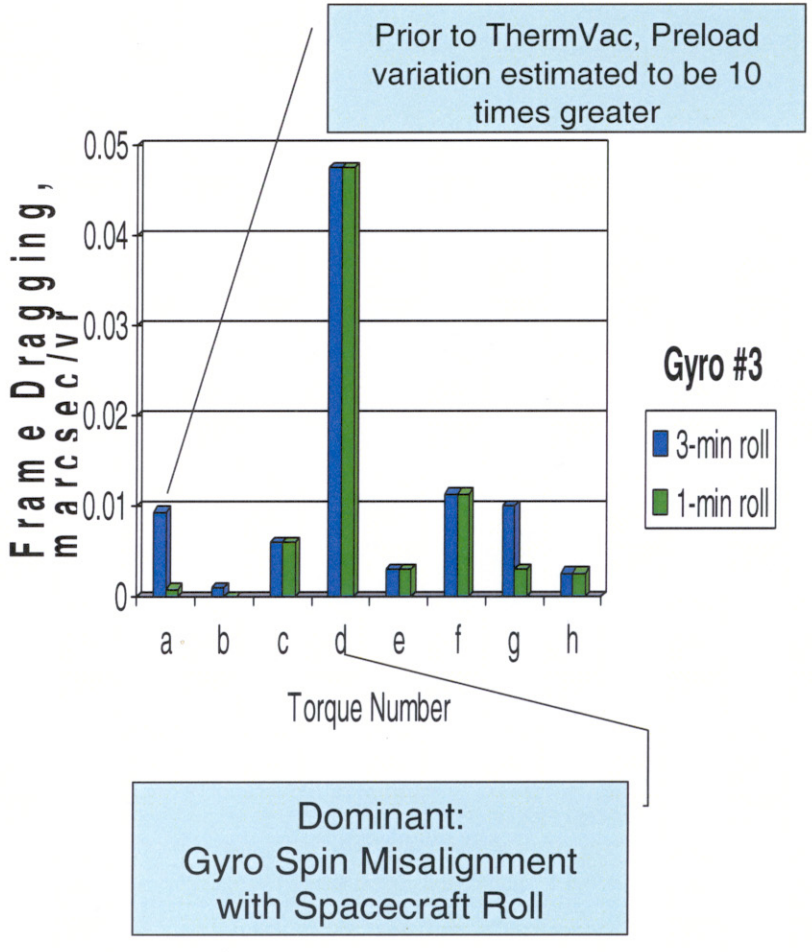

I. SUPPORT-DEPENDENT TORQUES FROM TEMPERATURE VARIATONS OF SUSPENSION ELECTRONICS AT SPACECRAFT ROLL-RATE (a, b, g)

- a: roll-variation of preload voltage difference (hA - hB)
- b: roll-variation of sensing bridge voltages
- g: fixed sums of preload (hA + hB, hC) plus roll-variation of rotor miscentering

Note: Temperature variations of electronics measured on orbit.

II: SUPPORT-DEPENDENT TORQUES FROM NON-TEMPERATURE DEPENDENT EFFECTS (d, f, h)

- d: gyro spin misaligned with spacecraft roll (1 arc-s mean over year)
- f: net gravity-gradient acceleration in orbit plane from variations in altitude due to Earth's oblateness
- h: sagging of gyro at twice-orbit period due to Earth's gravity gradient

III. SUPPORT-INDEPENDENT TORQUES (c, e)

- c: London moment coupling to local magnetic shield – gyro axis misaligned with line-of-sight to star
- e: Earth's gravity gradient on gyro oblateness

Geodetic: Top Eight Classical Gyro Disturbance Terms *(ALL TERMS > 0.001 MILLIARC-SEC/YEAR)*

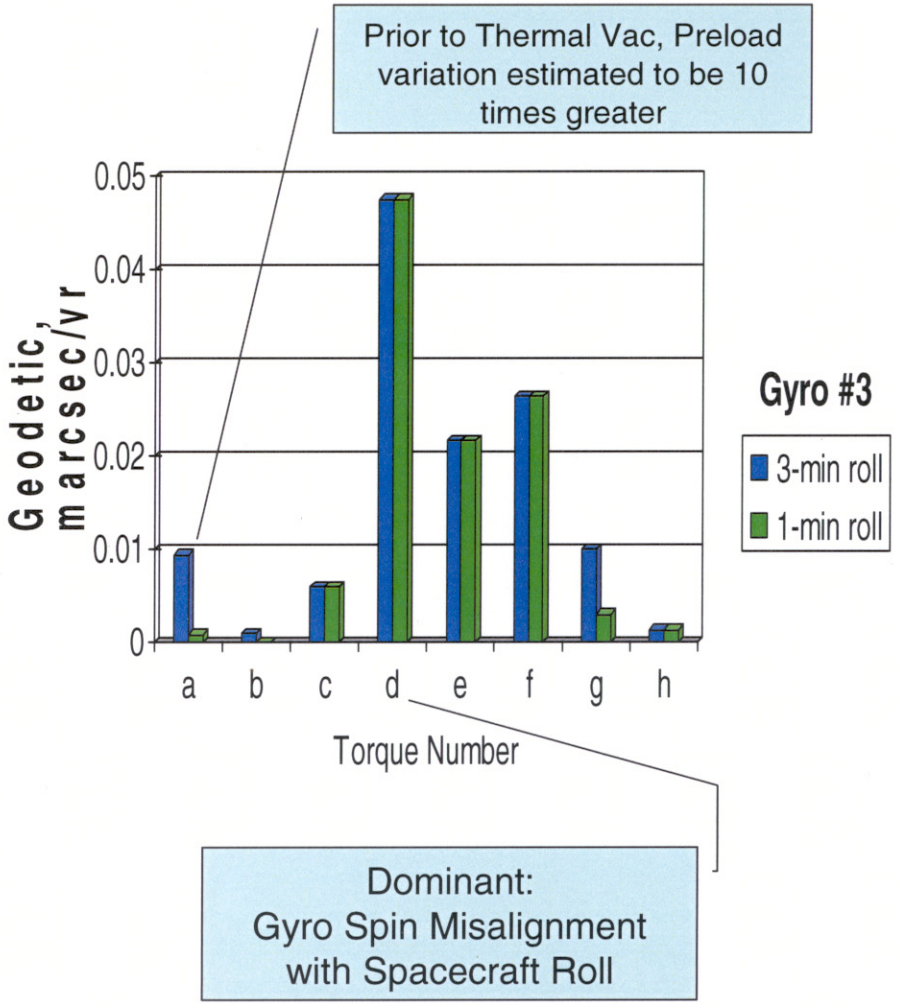

I. SUPPORT-DEPENDENT TORQUES FROM TEMPERATURE VARIATONS OF SUSPENSION ELECTRONICS AT SPACECRAFT ROLL-RATE (a, b, g)

- a: roll-variation of preload voltage difference (hA - hB)
- b: roll-variation of sensing bridge voltages
- g: fixed sums of preload (hA + hB, hC) plus roll-variation of rotor miscentering

Note: Temperature variations of electronics measured on orbit.

II: SUPPORT-DEPENDENT TORQUES FROM NON-TEMPERATURE DEPENDENT EFFECTS (d, f, h)

- d: gyro spin misaligned with spacecraft roll (1 arc-s mean over year)
- f: net gravity-gradient acceleration in orbit plane from variations in altitude due to Earth's oblateness
- h: sagging of gyro at twice-orbit period due to Earth's gravity gradient

III. SUPPORT-INDEPENDENT TORQUES (c, e)

- c: London moment coupling to local magnetic shield – gyro axis misaligned with line-of-sight to star
- e: Earth's gravity gradient on gyro oblateness

Readout Beats Requirement I: SQUID Noise

- Readout T002 Requirement ~ 0.3 marc-s/yr
  - allocated 0.2 marc-s/yr =
    SQUID noise density190 marc-s/√Hz @ 130 Hz spin speed, 3-min roll
- Measured noise in Payload testing [with full EMI/EMC qualification

July 2001

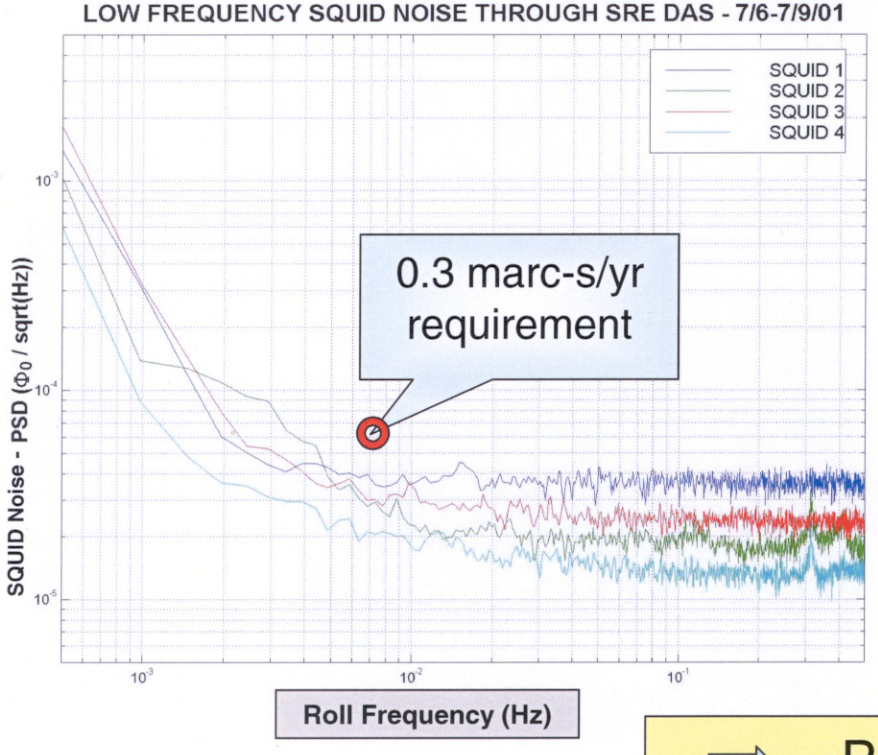

Actual SQUID Noise: 120 - 148 marc-s/√Hz

Measured spin speeds: 127, 151, 128, 147 Hz

⇨ Performance at different roll rates

EXPERIMENT ERROR
POLAR ORBIT, SEPT LAUNCH

STANFORD
Lockheed

LMSC-F277281-4
22 February 1991

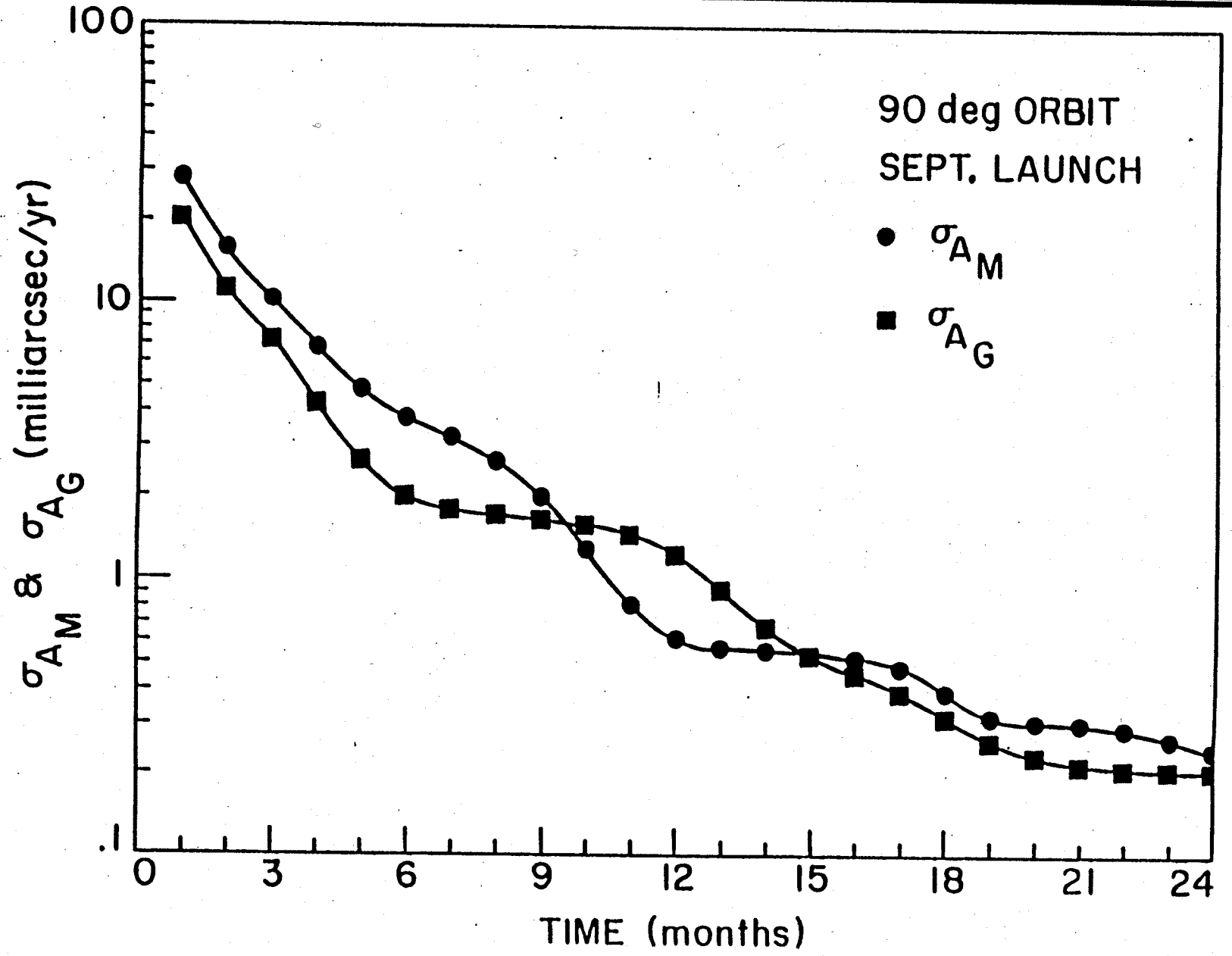

GP-B Final 4-Gyro Disturbance and Readout Performance

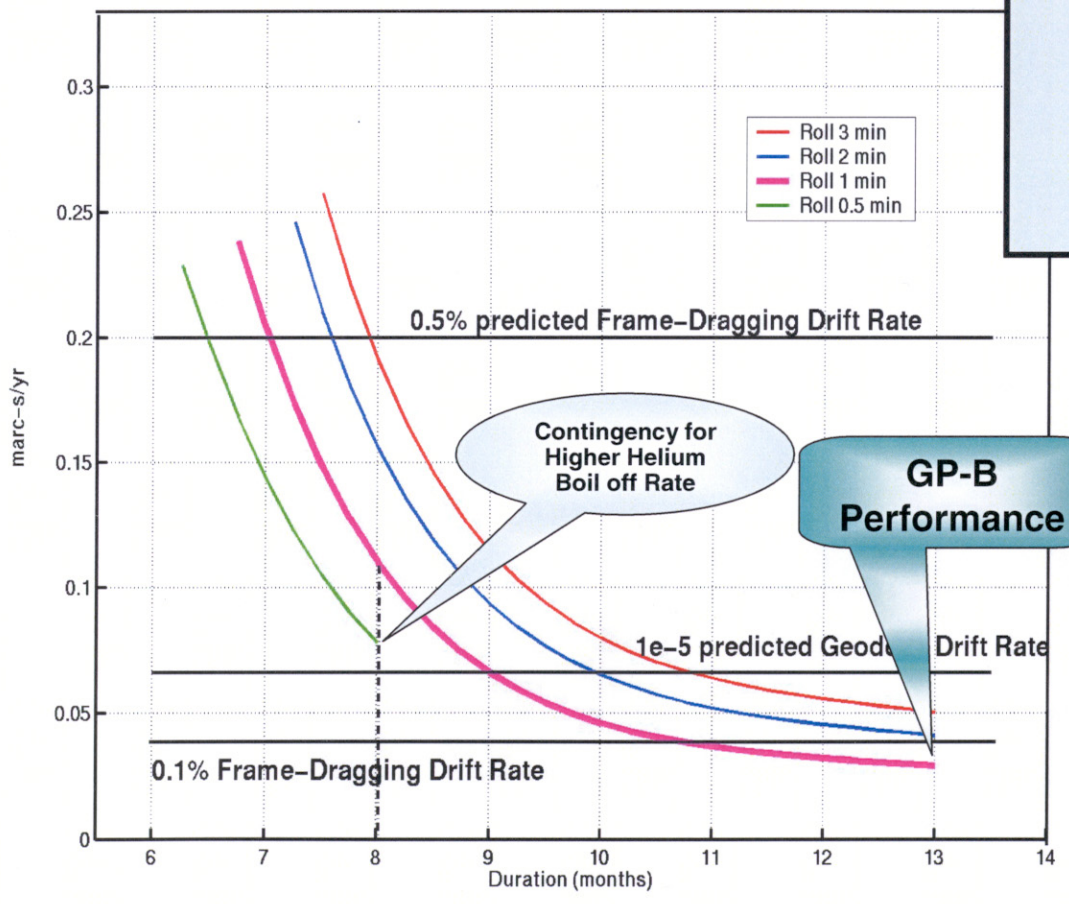

- **13-month science data**
- **1-min roll**
- **4-gyro mean**

0.038 marc-s/yr

To which add uncertainty in Guide star proper motion

Current Limiting Systematic Errors in Proper Motion Measurement (courtesy CfA)

	marc-s/yr
• VLBI effects	
– structure in reference sources	< 0.05
– radio emission drift from star	< 0.03
– additional companion	< 0.01
• Optical effects (geometrical dia of star 1.3 marc-s)	
– guide star variability + nebulosity gradient	< 0.02
– guide star variability + zodiacal light	< 0.002
– guide star variability + additional star	< 0.03
– star spot motion	< 0.02


GP-B

GPB TECHNICAL INNOVATION

Cryogenics in space: superfluid Helium

IRAS and COBE beneficiaries

Reduction of disturbance torques

Round gyro balls: reduction of quadrupole coupling

Drag free operation: "zero" g orbit, efflux gas actuation

Charge compensation of gyro rotor

LISA (Laser Interferometer Space Antenna) beneficiary

Retention of spherical symmetry

London moment readout: ultra low B fields

Electric centering servo (Nordsieck gyro)

Gas spin up

Long term geometric stability

Cryogenic operation: reduction of creep

Monolithic fused quartz construction: catalysis bonding

Precision low noise mechanical experiments beneficiaries

NEW PRECEDENTS SET BY GPB

A physics experiment carried out in space: vary parameters

vary charge

vary centering potential

vary spin rate of satellite

four gyro with different spin direction

measurement of perturbing torque at low gyro spin

Calibration

Measure deflection of starlight using gyro reference

Measure aberration of starlight (parallax to guide star)

Offset guide from another star with known proper motion

Fundamental problem with GR experiment

How to avoid the iteration to the "expected" result

Follow on

LAGEOS complementary orbit Lense-Thirring measurement

Kerr Black Hole binaries: gravitational wave inverse solutions